



Italian National Agency for New Technologies, Energy and Sustainable Economic Development

<http://www.enea.it/en>

<http://robotica.casaccia.enea.it/index.php?lang=en>

This paper is a pre-print. The final paper is available on:

Polymer network and blends: „Influence of molecular weight and molecular weight distribution on crystallization and thermal behaviour of isotactic polypropilene“, M. Avella, R. dell’Erba, L. D’Orazio and E. Martuscelli 5 (1), 47-54, 1995

Influence of Molecular Weight and Molecular Weight Distribution on Crystallization and Thermal Behavior of Isotactic Polypropylene

Maurizio Avella, Ramiro dell'Erba, Loredana D'Orazio, and Ezio Martuscelli

Istituto di Ricerche e Tecnologia delle Materie Plastiche, C.N.R., Via Toiano 6, 80072 Arco Felice (Napoli), Italy

Differential Scanning Calorimetry (D.S.C.) and Optical Microscopy have been used in order to assess the influence of molecular weight and molecular weight distribution (MWD) on thermal behavior and crystallization process of isotactic polypropylene (iPP) samples, all characterized by very high isotacticity index (98 wt%).

The values of the equilibrium melting temperature (T_m) and surface free energy of folding (σ_e) of iPP lamellar crystals have been determined according to the kinetic theory of polymer crystallization. Such thermodynamic parameters were found to increase with increasing iPP molecular weight, for a given iPP MWD and to decrease with increasing iPP MWD, for a given iPP molecular weight. Also the values of the radial growth rate of iPP spherulites and nucleation density were found to be affected noticeably by molecular weight and MWD of iPP. For a given undercooling, ΔT , G decreases strongly with increasing iPP molecular weight. On the other hand faster nucleation was shown by iPP samples with comparatively lower molecular weight and broader MWD.

Keywords: Catalyst; Crystallization; Melting; Molecular Weight; Nucleation Density; Polypropylene

INTRODUCTION

In a previous paper we studied the influence of stereochemical composition on the crystallization and thermal behavior of iPP samples synthesized with different catalyst systems (low, high, and very high yield) by HIMONT ITALIA.¹ The crystals obtained from the isothermal crystallization of such samples have shown values of equilibrium melting temperature (T_m), free energy of nucleation ($\Delta\Phi^*$), and surface free energy of folding (σ_e) to be strongly dependent upon the amount and distribution of configurational irregularities existing along the chains and upon the molecular weight distribution.

In order to assess the influence of molecular weight and molecular weight distribution (taken as polydispersity) on the thermal behavior and on the isothermal crystallization process of the iPP, we studied iPP samples all characterized by the same very high isotacticity index (98 wt%) and, having for a given MWD, different molecular weight, and, for a given molecular weight, different MWD. The synthesis of such kind of iPP samples was carried out by HIMONT by means of a new process patented by HIMONT, that use advanced superactive catalyst systems.²

In the present paper the results of the investigations performed according to the kinetic theory of polymer crystallization³⁻⁷ on thermal behavior, radial growth rate of spherulites, nucleation density, overall rate of crystallization, and morphology of such iPP samples are reported. The final target of the work is a deeper understanding of relationships between molecular structure of iPP and its properties.

EXPERIMENTAL

MATERIALS

Five different samples of isotactic polypropylene (iPP), supplied by HIMONT ITALIA, were investigated.

Some of the molecular and physical characteristics of the samples are listed in the Tables 1 and 2, respectively.

Table 1: Molecular weights obtained by GPC in ODCB at 135°C

| Sample | M_n | M_w | M_z | M_w/M_n |
|--------|-------|--------|---------|-----------|
| iPP1 | 17200 | 111000 | 545000 | 6.4 |
| iPP2 | 17900 | 172000 | 930000 | 9.6 |
| iPP3 | 52900 | 361000 | 2332000 | 6.8 |
| iPP4 | 66600 | 446000 | 2406000 | 6.7 |
| iPP5 | 91000 | 729000 | 3852000 | 8.0 |

A control of the isotacticity index of the various iPP samples was measured by 50.32 MHz ¹³C NMR. The solvent used for iPP was: 1,2,4-trichlorobenzene + 15% tetrachlorodideuteroethane (v/v) and the spectra were run at 110°C over 24 hrs.

The results have shown, for all iPP samples, an isotacticity index equal to 98±1%, thereby excluding an eventual influence of the tacticity on the crystallization and thermal behavior of iPP.

PROCEDURES

Thermal analysis and crystallization kinetics

The kinetics of isothermal crystallization from melt, of all samples were studied by using a Mettler TA3000 (dsc-30) DSC operating under nitrogen atmosphere.

The following procedure was used: the samples were kept for 10 minutes at 200°C and then cooled (50°C/min) to crystallization temperature T_c . The dH/dt evolved during the isothermal crystallization was recorded as

Table 2: Characteristics of iPP samples as obtained by polymerization

| Sample | Melt flow rate (g min ⁻¹) | η (135°C) | Flexural modulus ASTM D790 (N mm ⁻²) | Izod strength ASTM D256 | Hardness Rockwell ASTM D785 | Vicat (ion) ASTM D1525 | HDT (°C) |
|--------|--|----------------|--|----------------------------|--------------------------------|---------------------------|-------------|
| iPP1 | 390.0 | 0.76 | 1600 | 20 | 96 | 156 | 98 |
| iPP2 | 90.0 | 0.97 | 1600 | 20 | 96 | 156 | 98 |
| iPP3 | 5.7 | 1.72 | 1550 | 40 | 95 | 155 | 98 |
| iPP4 | 2.0 | 2.07 | 1500 | 60 | 92 | 154 | 95 |
| iPP5 | 0.3 | 2.36 | 1450 | 100 | 90 | 153 | 93 |

Table 3: Values of melting temperature, T'_m , crystallinity index, X_c , and glass transition temperature, T_g , for samples of iPP as obtained from synthesis

| Sample | T'_m (°C) | X_c (%) | T_g (°C) |
|--------|-------------|-----------|------------|
| iPP1 | 167 | 35 | -6 |
| iPP2 | 166 | 34 | -9 |
| iPP3 | 165 | 30 | -9 |
| iPP4 | 164 | 29 | -10 |
| iPP5 | 160 | 27 | -7 |

function of t , and the weight fraction X_t of material crystallized after the time t was determined from the relation:

$$X_t = \frac{\int_0^t \frac{dH}{dt} dt}{\int_0^\infty \frac{dH}{dt} dt}$$

The first integral is the crystallization heat evolved at the time t , while the second is the total crystallization heat.

The melting temperature, T'_m , and the apparent enthalpy of fusion, ΔH_m^* , of each sample, after isothermal crystallization at T_c , were measured from the maximum and the area of DSC endotherm, respectively, obtained by heating the samples directly from T_c to 200°C with heating rate of 10°C/min.

The temperature of the calorimeter was calibrated versus the melting points of high purity standards with precision of $\pm 0.2^\circ\text{C}$.

The crystallinity fraction, X_c , of the samples were determined at each T_c by the ratio ΔH_m^* to the melting enthalpy ΔH_m of a sample with 100% of crystallinity taken as 209 J/g.⁸

To determine the glass transition temperature, the following procedure was used: after a preliminary melting at 200°C for 10 min the samples were quickly cooled (50°C/min) to -100°C and then heated to 200°C at a heating rate of 20°C/min.

The heat dH/dt , evolved during the scanning process, was recorded as a function of temperature. The T_g of the sample was taken as the temperature corresponding to the flex point of the curve when the transition is equal to 50%.

Optical Microscopy

An optical polarizing Leitz microscope equipped with a Mettler hot stage was used to determine the radial growth rates, G , of iPP spherulites isothermally crystallized at different temperatures, T_c . The hot stage could be held at fixed temperature within $\pm 0.2^\circ\text{C}$ of precision.

The following procedure was used: iPP films were sandwiched between a microscope slide and a cover glass, heated at 200°C and kept at this temperature for 10 min to destroy any traces of crystallinity, then the temperature was rapidly lowered to a prefixed T_c and the iPP samples allowed to crystallize isothermally.

Photomicrographs of growing spherulites were taken at appropriate time intervals. The radii of spherulites, r , were measured from the photos, and G was calculated as slope of the linear plot against the time. Finally micrographs were taken at completed crystallization to carry out the measurements of the nucleation density of the spherulites.

RESULTS AND DISCUSSION

THERMAL PROPERTIES OF iPP AS OBTAINED FROM SYNTHESIS PROCESS

The melting point, T'_m , the crystallinity index, X_c , and the glass transition temperature, T_g , for all the samples under investigation are reported in Table 3. The iPP were treated as received from the synthesis process.

As shown, for almost the same value of MWD (look at iPP1, iPP3, and iPP4 samples), the T'_m and X_c values tend to decrease with increasing iPP molecular weight. No

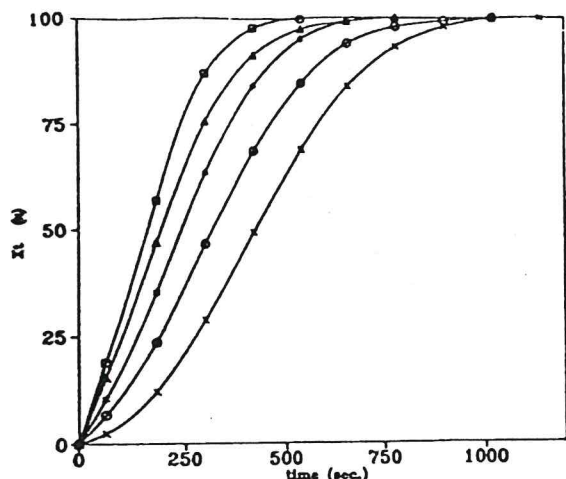


Figure 1. Isothermal curves of crystallization for iPP1 sample at $T_c = 398$ K (\square); 399 K (Δ); 400 K ($*$); 401 K (O); 402 K ($+$).

relevant dependence of T'_m and X_c values upon the MWD value (look at iPP1 and iPP2 samples) is, on the other hand, found.

T_g values, are only slightly affected by iPP molecular weight and MWD. Such finding indicates that there is a slight influence of the molecular motions of the chain-end segments on the T_g of such iPP. In other words it can be deduced that in the curve representing the dependence of T_g on the molecular weight of polymer, the molecular weight of an iPP samples is to be located in the plateau region.⁹

ISOTHERMAL BULK CRYSTALLIZATION

The isothermal curves of crystallization were obtained by plotting, at constant T_c , the crystalline fraction at time t (X_t) against the time.

An example of crystallization isotherm for iPP1 sample is shown in Figure 1. From this curve the half time of crystallization, $t_{0.5}$, defined as the time taken for half of the crystallinity to develop, is obtained.

The half time, $t_{0.5}$, for all the samples investigated, as function of crystallization temperature T_c is reported in Figure 2a.

From the examination of these trends, it emerges that, for a given T_c , the values of $t_{0.5}$ increase with increasing the molecular weight of iPP samples characterized by almost the same MWD values (iPP1, iPP3, and iPP4) and increase with decreasing MWD of iPP samples characterized by almost the same M_n values (iPP1 and iPP2). This effect becomes larger with reducing undercooling. For high undercooling in fact, it can be observed that the values of $t_{0.5}$ tend to coalesce and this can be accounted for by assuming that the diffusion term becomes predominant (see also Figure 2b where the $t_{0.5}$ of iPP samples as function of undercooling ΔT are reported: $\Delta T = T_m - T_c$ where T_m is the equilibrium melting temperature). The

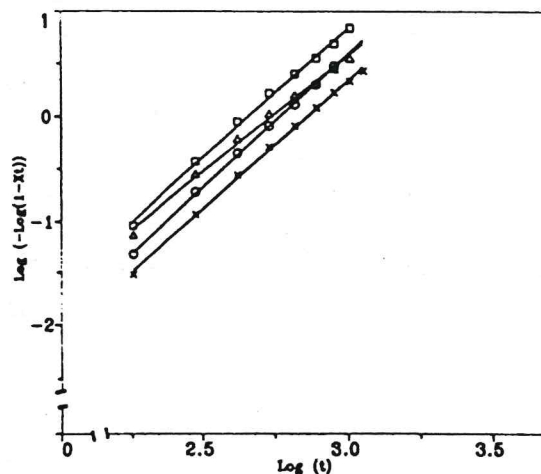
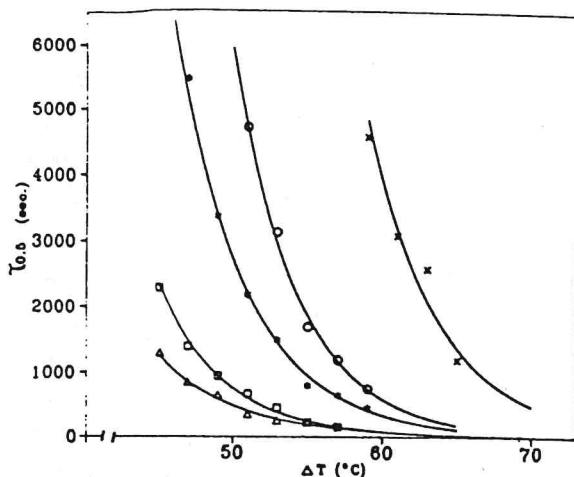
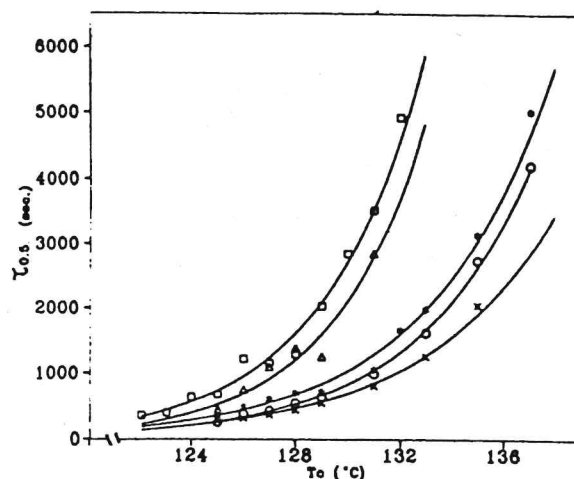


Figure 2. Half time of crystallization, $t_{0.5}$ of all samples versus (a) crystallization temperature, T_c ; (b) undercooling $\Delta T = T_m - T_c$; iPP1 (\square); iPP2 (Δ); iPP3 ($*$); iPP4 (O); iPP5 ($+$).

analysis of the crystallization kinetics, for each T_c , has been carried out on the basis of the Avrami equation:³

$$1 - X_t = \exp(-knt^n) \quad [1]$$

Table 4: Half-time of crystallization, $t_{0.5}$, Avrami Index, and overall kinetic rate constant, K_n , of iPP samples as a function of crystallization temperature

| Sample | T_c (°C) | $t_{0.5}$ (s) | n | K_n (s ⁻ⁿ) |
|--------|------------|---------------|-----|--------------------------|
| iPP1 | 125 | 278 | 2.6 | 3.6E-7 |
| | 126 | 313 | 2.3 | 1.3E-5 |
| | 127 | 362 | 2.5 | 2.3E-7 |
| | 128 | 439 | 2.4 | 2.6E-7 |
| | 129 | 544 | 2.9 | 9.2E-9 |
| | 131 | 808 | 3.0 | 1.8E-9 |
| | 133 | 1258 | 3.1 | 2.4E-10 |
| | 135 | 2047 | 3.1 | 3.5E-11 |
| iPP2 | 125 | 250 | 2.5 | 6.7E-7 |
| | 126 | 368 | 2.5 | 3.8E-7 |
| | 127 | 424 | 2.3 | 6.3E-7 |
| | 128 | 542 | 2.2 | 6.7E-7 |
| | 129 | 639 | 2.4 | 1.4E-7 |
| | 131 | 980 | 2.6 | 1.0E-8 |
| | 135 | 1620 | 2.6 | 3.1E-9 |
| | 137 | 2740 | 2.5 | 2.2E-9 |
| iPP3 | 127 | 600 | 2.7 | 3.0E-8 |
| | 128 | 898 | 2.6 | 2.1E-8 |
| | 131 | 1059 | 2.8 | 1.2E-8 |
| | 132 | 1657 | 3.1 | 8.3E-11 |
| | 133 | 1987 | 2.5 | 3.1E-9 |
| | 135 | 3144 | 2.8 | 1.7E-10 |
| | 137 | 5014 | 3.2 | 1.5E-12 |
| iPP4 | 125 | 437 | 3.5 | 2.9E-10 |
| | 126 | 751 | 2.8 | 7.0E-9 |
| | 127 | 1098 | 2.6 | 1.0E-8 |
| | 128 | 1383 | 2.4 | 2.2E-8 |
| | 129 | 1256 | 3.7 | 1.8E-12 |
| | 131 | 2647 | 2.8 | 1.7E-7 |
| iPP5 | 122 | 353 | 3.3 | 3.4E-9 |
| | 123 | 392 | 3.4 | 9.9E-10 |
| | 124 | 634 | 3.4 | 2.3E-10 |
| | 125 | 874 | 3.2 | 5.7E-10 |
| | 126 | 1220 | 3.0 | 4.1E-10 |
| | 128 | 1294 | 3.7 | 2.4E-12 |
| | 129 | 2035 | 3.5 | 1.8E-12 |
| | 130 | 2845 | 3.4 | 1.3E-12 |
| | 131 | 3520 | 3.5 | 1.9E-13 |

where kn ($= \ln 2 / (t_{0.5})^n$) is the kinetic rate constant and n is a parameter depending on the geometry of the growing crystals and the nucleation process.

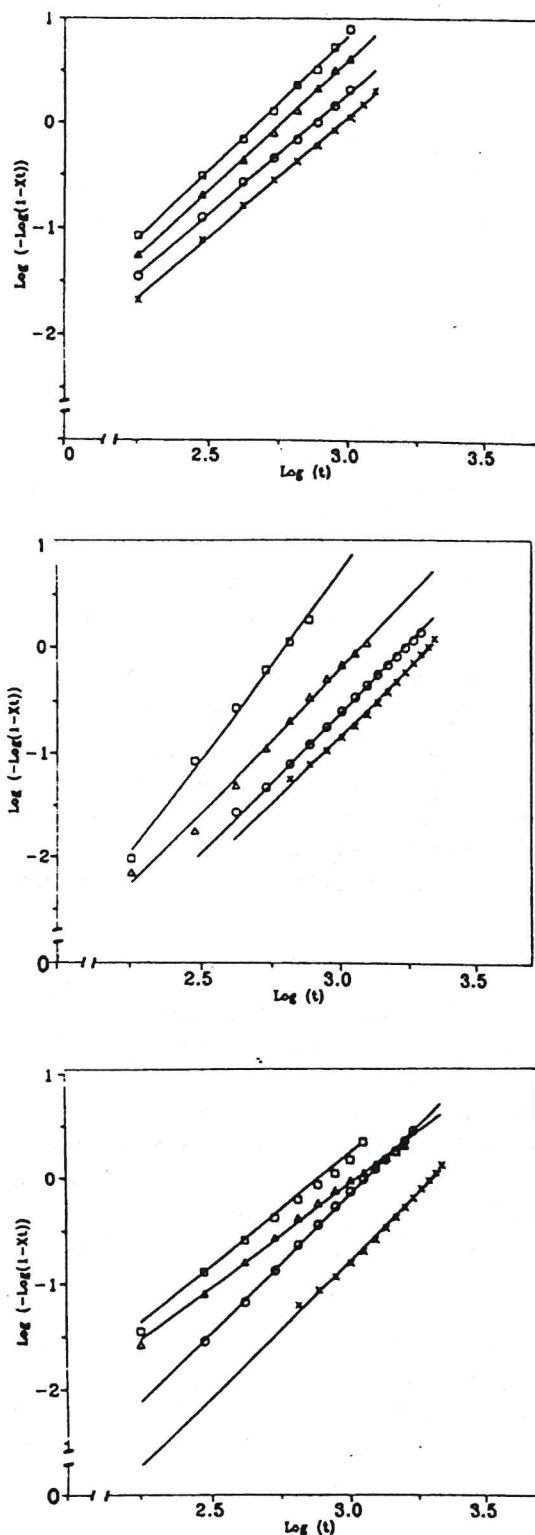


Figure 3. Avrami plots for (a) iPP1; (b) iPP2; (c) iPP3; (d) iPP4; (e) iPP5. $T_c = 398$ K (\square); 399 K (Δ); 400 K (\circ); 401 K (\times).

The values of n and kn were calculated from the slope and the intercept, respectively, of the straight line obtained by plotting the quantity $\log(-\log(1-X_t))$ against $\log t$ (see Figure 3 a-e).

Table 5: Values of equilibrium melting temperature, T_m , and constant, γ , for various iPP samples

| Sample | T_m ($^{\circ}\text{C}$) | γ (± 0.2) |
|--------|------------------------------|------------------------|
| iPP1 | 181 | 2.9 |
| iPP2 | 178 | 3.4 |
| iPP3 | 184 | 3.0 |
| iPP4 | 185 | 2.8 |
| iPP5 | 191 | 2.4 |

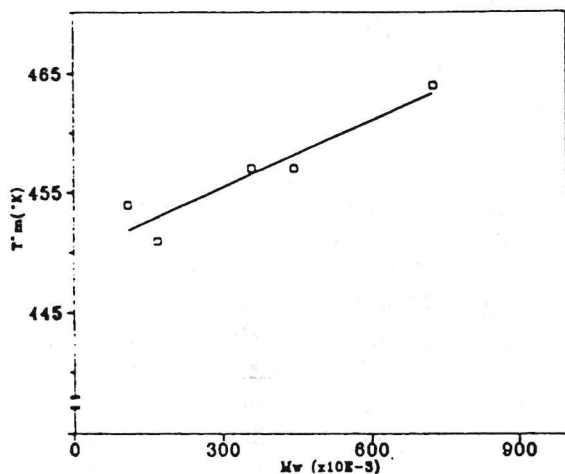


Figure 4. Equilibrium melting temperature, T_m , versus molecular mass of the samples.

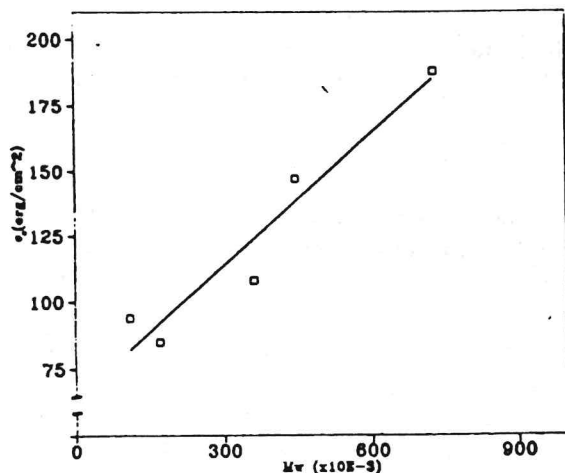


Figure 5. Surface free energy of folding, σ_e , as a function of molecular mass of the samples.

In Table 4 the values of k_n and n for all T_c investigated, are shown.

No relevant dependence of the Avrami exponents on the iPP molecular weight and MWD can be found. As a

matter of fact, the values of Avrami index range around 3. Such value is in agreement with literature data^{4,10,11} indicating that the crystallization process of iPP is characterized by a heterogeneous nucleation and by a three-dimensional growth of crystals.⁵

MELTING BEHAVIOR

DSC thermograms of isothermally crystallized iPP present only one fusion peak corresponding to the a form of the iPP. The melting temperature T'_m of all investigated iPP samples increases linearly with T_c according to the Hoffman-Weeks relation:⁶

$$T'_m = T_m(\gamma - 1)/\gamma + T_c/\gamma \quad [2]$$

where T_m is the equilibrium melting temperature, (i.e., the melting temperature of a crystal with infinite thickness and no defects⁵), and γ is a constant determined by the ratio between the final thickness of the crystalline lamellae of the spherulites crystallized at T_c , after a certain time, and the initial critical thickness⁴ (see Table 5).

The values of T_m and γ were calculated by extrapolation of the T'_m versus T_c line to the line of equation $T'_m = T_c$ and from the slope respectively. The values of T_m and of the morphological factors, γ , are reported in Table 5.

As shown, for a given MWD, the equilibrium melting point tends to increase with increasing the molecular weight of iPP (look at iPP1, iPP3, and iPP4 samples) whereas, for a given molecular weight, the equilibrium melting point decreases with increasing MWD (look at iPP1 and iPP2 samples). The last finding supports observation that increasing MWD increases the presence of defects along iPP chain. The highest γ value found for iPP2 sample is a confirmation: a large γ , in fact, indicates a more pronounced phenomenon of perfecting of existing crystals following an annealing at the examined T_c .

NUCLEATION CONTROL OF CRYSTALLIZATION RATE

According to the kinetic theory of crystallization¹², the temperature dependence of the overall rate constant k_n may be written as:

$$\alpha = \frac{1}{n} \log k_n + \frac{U^*}{2.3R(T_c - T_\infty)} = \log A - \frac{k_g}{2.3T_c \Delta T f} \quad [3]$$

where A is a constant; the $U^*/2.3R(T_c - T_\infty)$ term contains the energetic contribution of diffusional process of the amorphous and crystallizable material to the overall kinetic constant k_n ; U^* is the activation energy for the transport process in the melt at the liquid solid interface, T_∞ ($T_\infty = T_g - C$ with C a constant), is the temperature below which the motion ceases. The factor f is a correction term that takes into account the temperature dependence of the melting enthalpy ΔH_m and is given empirically as $f = 2T_c/T_m + T_c$.

Table 6: Radial growth rate, G , of iPP spherulites as a function of undercooling, ΔT

| Sample | G (μmin) | | |
|--------|-------------------------|-----------------|-----------------|
| | $\Delta T = 55$ | $\Delta T = 60$ | $\Delta T = 65$ |
| iPP1 | 16.1 | 49.6 | 52.6 |
| iPP2 | 7.3 | 17.8 | 38.5 |
| iPP3 | 0.8 | 2.4 | 7.0 |

Table 7: Number of primary nuclei \times unit volume (cm^3), \bar{N} , as a function of undercooling, ΔT

| Sample | $\bar{N} \times \text{unit volume} (\text{cm}^3)$ | | |
|--------|---|-----------------|-----------------|
| | $\Delta T = 55$ | $\Delta T = 60$ | $\Delta T = 65$ |
| iPP1 | 9E5 | 8E6 | 4E6 |
| iPP2 | 7E4 | 5E5 | 5E5 |
| iPP3 | 2E3 | 1E6 | 4E5 |

The term k_g is the free energy of formation of a nucleus of critical dimension,⁴ $\Delta T (=T_m - T_c)$ is the undercooling.

Straight lines were obtained by plotting the α expression versus $1/2.3T_c\Delta T$. The best fit of our experimental data is obtained by setting $C = 30$ and $U^* = 4120$ cal/mol; from the slopes the numerical values of k_g were calculated.

Application of the Z test of Lauritzen¹³ seems to indicate that for our iPP, the crystallization process conforms to regime I. In this case the expression for k_g is:

$$k_g = \frac{4b_o\sigma\sigma_e T_m}{\Delta H_m k} \quad [4]$$

where k is the Boltzmann constant, ΔH_m the melting enthalpy, σ and σ_e lateral and folding surface free energies, and T_m the equilibrium melting temperature.

Using for b_o and ΔH_m the following literature values: $b_o = 0.525 \text{ nm}^{14}$ and $\Delta H_m = 209 \text{ J/g}$,⁸ and $\sigma = 0.1b_o\Delta H_m$, it is possible to calculate the surface energy of folding, σ_e . As shown in Figure 5 the values of σ_e increase with increasing iPP molecular weight, for iPP samples with almost the same MWD. On the other hand it seems that the σ_e values tend to decrease with increasing MWD for iPP samples with comparable molecular weights.

The folding surface free energy, σ_e , can be expressed by the fundamental thermodynamic equation:⁷

$$\sigma_e = \Delta H_e - TS_e \quad [5]$$

where ΔH_e is the folding surface enthalpy and S_e the folding surface entropy. By considering that the enthalpy values of examined iPP were taken as constant, the σ_e variation can be attributed to a variation of S_e term.

Therefore, for a given MWD, by increasing the molecular weights, we obtain iPP crystals with a more regularly folded surface due to a diminution of entropy. However, in the case of iPP samples characterized by a broader MWD, for comparable molecular weights, the observed decrease in σ_e values could be due to an increase of S_e term.

RADIAL GROWTH RATE AND NUCLEATION DENSITY OF SPHERULITES

The values of the radial growth rate, G , measured on thin films of three samples, iPP1, iPP2, and iPP3, as a function of the three different undercooling ΔT values (55, 60, and 65°C) are listed in Table 6; the ΔT were calculated by using the equilibrium melting temperatures obtained by DSC experiments (see Table 5).

It can be observed that, for a given sample, G increases with the increasing of ΔT (at least in the range of T_c examined). Moreover, for the same value of ΔT , it is to be pointed out that G decreases with increasing of the molecular weight of iPP samples having almost the same MWD. A less pronounced decrease in G values, for given ΔT , is also shown by iPP samples with comparatively higher MWD for almost constant molecular weight (look at iPP1 and iPP2 samples). These latter observations can be related to the findings reported in Figure 2b where is shown that the $t_{0.5}$ values of the various iPP, at a fixed ΔT , increase with increasing the molecular weight and decreasing MWD. Since $t_{0.5}$ is inversely proportional to k_n ,⁷ decrease in the overall kinetics is obtained with the increasing of the molecular weight and decreasing MWD.

By assuming a three-dimensional spherical growth with a instantaneous nucleation, the kinetic rate constant k_n can also be expressed by the following relation:⁴

$$K_n = (4/3)\pi G^3 \rho_c / \rho_a (1 - \lambda) \bar{N} \quad [6]$$

where ρ_c and ρ_a are the density of crystalline and amorphous region, respectively, λ is the fraction of crystallized material at $t = \infty$ and \bar{N} is the number of primary nuclei per unit volume.

By using the Eq 6 we calculated the \bar{N} values as function of undercooling and the findings are reported in Table 7. As shown, \bar{N} increases with increasing undercooling, ΔT , and, for a given ΔT , \bar{N} decreases with increasing of iPP molecular weight and MWD.

Figures 6 a-d show optical micrographs, taken at crossed polars, of the films of the spherulitic texture of two iPP samples (iPP1 and iPP3) crystallized at two different undercooling and precisely:

- Figure 6 a: iPP1 at $\Delta T=55$;
- Figure 6 b: iPP1 at $\Delta T=60$;
- Figure 6 c: iPP3 at $\Delta T=55$;
- Figure 6 d: iPP3 at $\Delta T=60$.

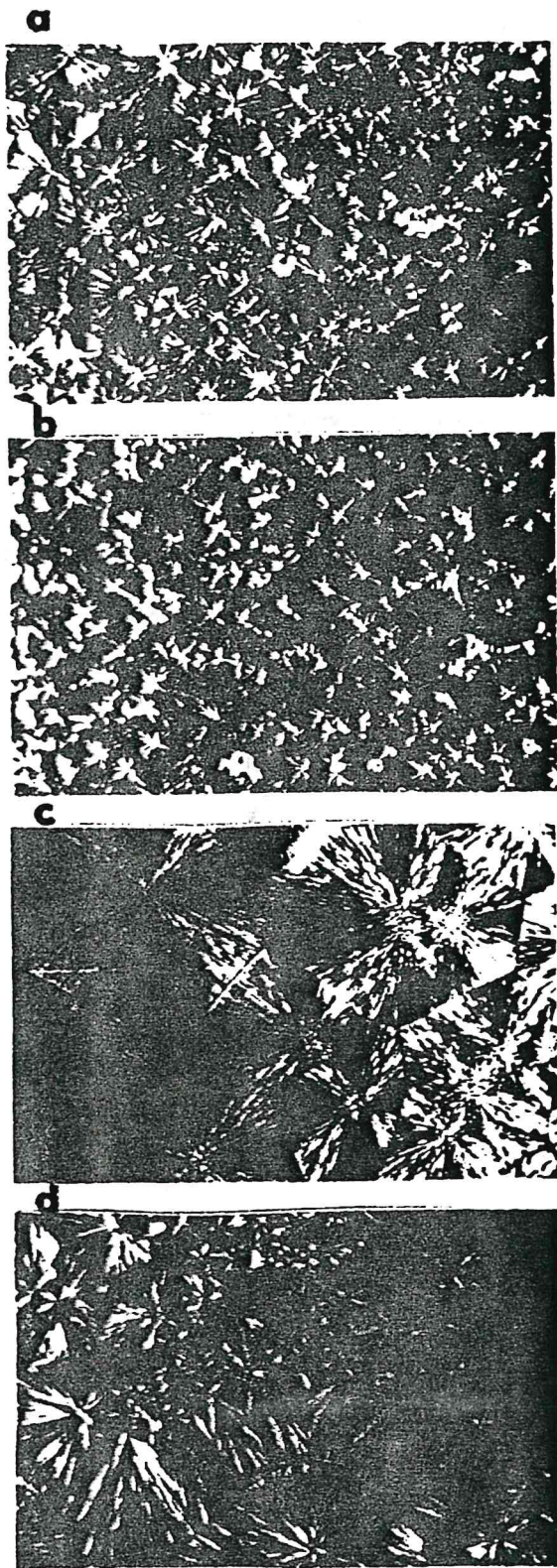


Figure 6. Optical micrographs for iPP samples: (a) iPP1 $\Delta T=55$; (b) iPP1 $\Delta T=60$; (c) iPP3 $\Delta T=55$; (d) iPP3 $\Delta T=60^\circ\text{C}$.

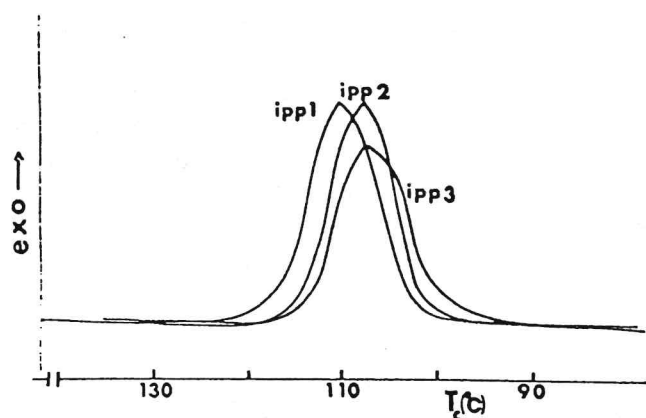


Figure 7. Crystallization peaks for iPP1, iPP2, iPP3 in non-isothermal experiments (scan rate $10^\circ\text{C}/\text{min}$).

The iPP sample, having comparatively lower molecular weight (iPP1), contains, for a given ΔT , a number of spherulites per unit surface higher than that observed for iPP sample, having higher molecular weight (iPP3).

A further evidence of the influence of the molecular weight on nucleation process can be assessed from the following non-isothermal DSC experiment. The iPP1 and iPP3 samples, after a melting at 200°C for 10 minutes, were cooled by using a scan rate of $10^\circ\text{C}/\text{min}$ (see Figure 7). From the trend of curves, a decrease of T_c (measured as maximum of crystallization peak) as function of the increase of M_w , indicating a faster nucleation of the samples with low molecular weight.

CONCLUDING REMARKS

A study, dealing with the influence of molecular weight and molecular weight distribution on crystallization process, thermal behavior, and morphology of iPP samples, all having the same very high isotacticity index, has been carried out.

It was found that both T'_m and X_c values decrease with increasing iPP molecular weight, irrespective of iPP MWD. Moreover, with reducing undercooling, the values of $t_{0.5}$ increase with increasing the iPP molecular weight, for a given iPP MWD. As far as the thermodynamic parameters, calculated according to the kinetic theory of polymer crystallization, both the T_m and σ_e values are found to increase with increasing iPP molecular weight, for a given iPP MWD and to decrease with increasing iPP MWD, for a given molecular weight.

Such findings can be accounted for by assuming that, in spite of the highest isotacticity index, there is a relevant influence of the low amount of configurational irregularities distributed along iPP chain: such irregularities de-

crease with increasing iPP molecular weight and with decreasing iPP MWD.

Also the values of the radial growth rate of spherulites and nucleation density are influenced by molecular weight and MWD of iPP. As a matter of fact, for a given ΔT , a strong decrease of the radial growth rate is found with increasing iPP molecular weight and with decreasing iPP MWD. Moreover a faster nucleation is shown by iPP samples with comparatively lower molecular weight and broader MWD indicating a nucleation effect of more defective iPP molecules during the crystallization process.

ACKNOWLEDGMENTS

The authors wish to express many thanks to Mr. E. Rossi for ^{13}C NMR characterization.

This work was partially supported by Progetto Finalizzato Chimica Fine II-C.N.R.

REFERENCES

1. E. Martuscelli, M. Avella, A. L. Segre, E. Rossi, G. Di Drusco, P. Galli, and T. Simonazzi, *Polymer*, **26**, 259 (1985).
2. P. Galli, T. Simonazzi, and D. Del Duca, *Acta Polymerica*, **39**, 81 (1988).
3. M. Avrami, *J. Chem. Phys.*, **7**, 1103 (1939).
4. L. Mandelkern in *Crystallization in Polymers*, Mc Graw-Hill, N.Y., 1964.
5. J. D. Hoffmann, *Spe. Trans.*, **4**, 315 (1964).
6. J. D. Hoffmann and J. J. Weeks, *J. Res. Natl. Bur. Stand.*, **66**, 13 (1962).
7. B. Wunderlich in *Macromolecular Physics*, Academic Press, N.Y., 1976.
8. J. Brandrup and E. M. Immergut in *Polymer Handbook*, Interscience Publication, N.Y., vol. 24, 1975.
9. L. Amelino and E. Martuscelli, *Polymer*, **16**, 864 (1970).
10. E. Martuscelli, M. Pracella, M. Avella, R. Greco, and G. Ragosta, *Macromol. Chem.*, **181**, 957 (1980).
11. E. Martuscelli, M. Avella, A. L. Segre, E. Rossi, G. Di Drusco, P. Galli, and T. Simonazzi, *Polymer*, **26**, 259 (1986).
12. J. D. Hoffmann, G. I. Davis, and Lauritzen in *Treatise on Solid State Chemistry*, Ed. Hanney, Plenum Press, N.Y., Vol. 3, 1976.
13. J. D. Hoffmann, *Polymer*, **24**, 3 (1983).
14. L. Crispino, E. Martuscelli, and M. Pracella, *Macromol. Chem.*, **181**, 1747 (1980).